MicroRNAs Control Intestinal Epithelial Differentiation, Architecture, and Barrier Function

LINDSAY B. MCKENNA,[*,‡] JONATHAN SCHUG,[*,‡] ANASTASSIOS VOUREKAS,[§] JAIME B. MCKENNA,[*,‡] NURIA C. BRAMSWIG,[*,‡] JOSHUA R. FRIEDMAN,[‖] and KLAUS H. KAESTNER[*,‡]

[*]Department of Genetics, [‡]Institute for Diabetes, Obesity, and Metabolism, and [§]Department of Pathology and Laboratory Medicine, Division of Neuropathology, University of Pennsylvania School of Medicine, Philadelphia; and [‖]Department of Pediatrics, Division of Gastroenterology, Hepatology, and Nutrition, University of Pennsylvania School of Medicine, Children's Hospital of Philadelphia, Philadelphia, Pennsylvania

BACKGROUND & AIMS: Whereas the importance of microRNA (miRNA) for the development of several tissues is well established, its role in the intestine is unknown. We aimed to quantify the complete miRNA expression profile of the mammalian intestinal mucosa and to determine the contribution of miRNAs to intestinal homeostasis using genetic means. **METHODS:** We determined the miRNA transcriptome of the mouse intestinal mucosa using ultra-high throughput sequencing. Using high-throughput sequencing of RNA isolated by cross-linking immunoprecipitation (HITS-CLIP), we identified miRNA-messenger RNA target relationships in the jejunum. We employed gene ablation of the obligatory miRNA-processing enzyme *Dicer1* to derive mice deficient for all miRNAs in intestinal epithelia. **RESULTS:** miRNA abundance varies dramatically in the intestinal mucosa, from 1 read per million to 250,000. Of the 453 miRNA families identified, mmu-miR-192 is the most highly expressed in both the small and large intestinal mucosa, and there is a 53% overlap in the top 15 expressed miRNAs between the 2 tissues. The intestinal epithelium of *Dicer1*$^{loxP/loxP}$;*Villin*-Cre mutant mice is disorganized, with a decrease in goblet cells, a dramatic increase in apoptosis in crypts of both jejunum and colon, and accelerated jejunal cell migration. Furthermore, intestinal barrier function is impaired in *Dicer1*-deficient mice, resulting in intestinal inflammation with lymphocyte and neutrophil infiltration. Our list of miRNA-messenger RNA targeting relationships in the small intestinal mucosa provides insight into the molecular mechanisms behind the phenotype of *Dicer1* mutant mice. **CONCLUSIONS: We have identified all intestinal miRNAs and shown using gene ablation of *Dicer1* that miRNAs play a vital role in the differentiation and function of the intestinal epithelium.**

Keywords: MicroRNA; miRNA; Intestinal Epithelium; Epithelial Barrier Function.

MicroRNAs (miRNAs) are 19–25 nucleotide (nt) single-stranded RNA molecules that modulate the activity of thousands of genes. miRNAs can decrease expression of target messenger RNA (mRNA) by binding to their 3′ untranslated regions (UTRs), leading to mRNA degradation, or by translational inhibition.[1] It has been proposed that more than one-third of human genes are regulated by miRNAs.[2]

The synthesis of mature miRNAs is complex. Primary miRNAs are transcribed by RNA polymerase II and cropped by the RNase III-type enzyme Drosha to a precursor miRNA (pre-miRNA), which forms an ~70 nt stem-loop structure.[3] Pre-miRNAs are cleaved by the RNase Dicer to form the mature and functional miRNA, which is loaded onto the Argonaute protein in the RNA-induced silencing complex (RISC).[3] Because Dicer is obligatory for miRNA processing, the inactivation of this gene by conditional gene ablation has been utilized to study miRNA function in several organ systems.[4–6] miRNAs play central roles in several important developmental and disease states ranging from larva formation in *Drosophila* to regulation of cancer progression in humans. In the intestine, thus far the main focus has been on the role of miRNAs in colorectal cancer.[7] In addition, specific miRNAs have been implicated in ulcerative colitis.[8]

The miRNA transcriptome of most organ systems is not known. Only a relatively shallow survey, with ~10 to 1000 miRNA sequences per tissue, has been reported based on sequencing of cloned miRNAs, capturing only the most abundantly expressed miRNAs.[9] The "colorectal microRNAome" also had a very limited sequencing depth because of technical limitations.[10] Thus, a comprehensive atlas of miRNAs expressed in the intestinal epithelium has not yet been reported.

Here, we report the comprehensive miRNA transcriptome of the intestinal mucosa of the mouse using ultra-high throughput sequencing. We also evaluated the contribution of miRNAs to intestinal differentiation and function using conditional gene ablation of *Dicer1*, the gene encoding the obligatory miRNA-processing enzyme,

Abbreviations used in this paper: BrdU, bromodeoxyuridine; miRNA, microRNA; mRNA, messenger RNA; NCBI, National Center for Biotechnology Information; nt, nucleotide; PCR, polymerase chain reaction; pre-miRNA, precursor miRNA; RISC, RNA-induced silencing complex; TUNEL, terminal deoxynucleotidyl transferase-mediated deoxyuridine triphosphate nick-end labeling; UTR, untranslated regions.

0016-5085/$36.00
doi:10.1053/j.gastro.2010.07.040

in the epithelium of the small and large intestine. Finally, we determined key miRNA-mRNA target relationships in the jejunal mucosa.

Materials and Methods

Identification and Quantification of miRNAs

Jejunal mucosa was scraped from the longitudinally sliced intestine of CD1 mice (n = 4), and small RNAs were isolated using the *mir*Vana miRNA kit (Ambion catalogue No. AM1560). Libraries were prepared using the Digital Gene Expression-Small RNA sample prep kit (Illumina, San Diego, CA, FC-102-1009) and sequenced on a Genome Analyzer II (Illumina). Trimmed reads were aligned to precursor miRNA sequence from miRBase (release 13.0), reference sequence (RefSeq) sequence (National Center for Biotechnology Information [NCBI], Bethesda, MD), and the mouse genome (mm8, NCBI build 36) with up to 2 mismatches using Illumina's efficient large-scale alignment of nucleotide databases (ELAND) aligner.

To compute expression levels, we grouped miRNA mature features into families when they shared a perfectly matching trimmed read with a length between 19 and 25 nt. Expression values were reported as the total number of trimmed reads that align to any member of the family with up to 2 mismatches. When trimmed reads hit multiple families, the counts for those reads were spread across the families in proportion to the number of unambiguously assigned reads. The average expression was calculated as the weighted average of the reads per million of the 2 technical replicates (25% each) and the biologic replicate (50%).

Mice

Dicer1^{loxP} mice[4] were a gift from Matthias Merkenschlager, and *Villin*-Cre mice[11] were kindly shared with us by Deborah Gumucio. Genotyping was performed by polymerase chain reaction (PCR) analysis using genomic DNA. All procedures involving mice were conducted in accordance with approved Institutional Animal Care and Use Committee protocols.

Expression Analysis

Dicer mRNA expression was measured using quantitative reverse-transcription polymerase chain reaction, as previously described.[12] miRNA levels were measured using the appropriate Taqman kits, using Sno202 as reference gene (mir-21 4373090, let-7b 4373168, Sno202 4380914; Applied Biosystems, Carlsbad, CA).

Histologic Analysis

Immunostaining was conducted as previously described[13] with the following antibodies and kits: CD3 1:200 (catalogue No. RM-9107: Labvision, Fremont, CA), CD45R 1:1000 (catalogue No. 550786: Pharmingen, San Diego, CA), Claudin-7 1:200 (catalogue No. Rb-10284: Labvision), Claudin-4 1:200 (catalogue No. 32-9400: Zymed, San Francisco, CA), BrdU 1:1000 (catalogue No. OBT0030G: Accurate, Westbury, NY), and Apoptag Plus peroxidase In Situ apoptosis kit (Millipore, Billerica, MA, S7101).

Microarray Analysis

Total RNA was isolated from small intestinal mucosa from control and *Dicer1*$^{loxP/loxP}$;*Villin*-Cre mice using the *mir*Vana miRNA kit (Ambion catalogue No. AM1560). Fifty nanograms of each RNA sample (4 pairs) were amplified and labeled using the Agilent QuickAmp kit (Agilent Technologies, Santa Clara, CA). Labeled samples were purified using the CGH Cleanup Column (Invitrogen, San Diego, CA) and hybridized overnight to the Agilent 4X44 Whole Mouse Genome Array. After hybridization the arrays were washed and scanned with the Agilent DNA microarray Scanner (Agilent Technologies). Median intensities of each element on the array were captured with Agilent Feature Extraction version 10.5 (Agilent Technologies).

The data were normalized by the print tip loess method using the Linear models for microarray data (LIMMA) package in R as described.[14] For statistical analysis, genes were called differentially expressed using the Significance Analysis of Microarrays one class response package with a false discovery rate of 10%[15] and a minimum fold change of 1.5×. Genes marked as absent, ie, with expression levels near background, were omitted. miRNA target predictions were downloaded from the miRBase Web site.[16]

Intestinal Permeability

Adult mice (n = 4) were fasted 3 hours and then gavaged with 500 μL of fluid containing unlabeled lactulose and mannitol (Sigma-Aldrich, St Louis, MO) at 5.5 mmol/L each in water and 10 μCi of [^{3}H] lactulose (1 mCi/mL) and 5 μCi of [^{14}C] mannitol (100 μCi/mL) (American Radiolabelled Chemicals, St Louis, MO). Fifteen microliters of plasma were collected via tail vein at various time points and [^{3}H] lactulose and [^{14}C] mannitol radioactivity determined by liquid scintillation counting.

High-Throughput Sequencing of RNA Isolated by Cross-Linking Immunoprecipitation (HITS-CLIP)

HITS-CLIP was performed as published using the monoclonal argonaute antibody 2A8.[17] Jejunal mucosa of CD1 mice (n = 4) was coarsely homogenized with a Dounce homogenizer and cross-linked 3 times on ice at 400 mJ/cm^2. The Illumina library was sequenced on an Illumina GA-IIx following standard protocols to a length of 38 base pairs to yield 20,943,291 reads. Trimmed reads were aligned to the mouse genome (NCBI Build 36/mm8), RefSeqs, and pre-miRNA (mirBase 13.0) using ELAND and allowing up to 2 mismatches. A total of

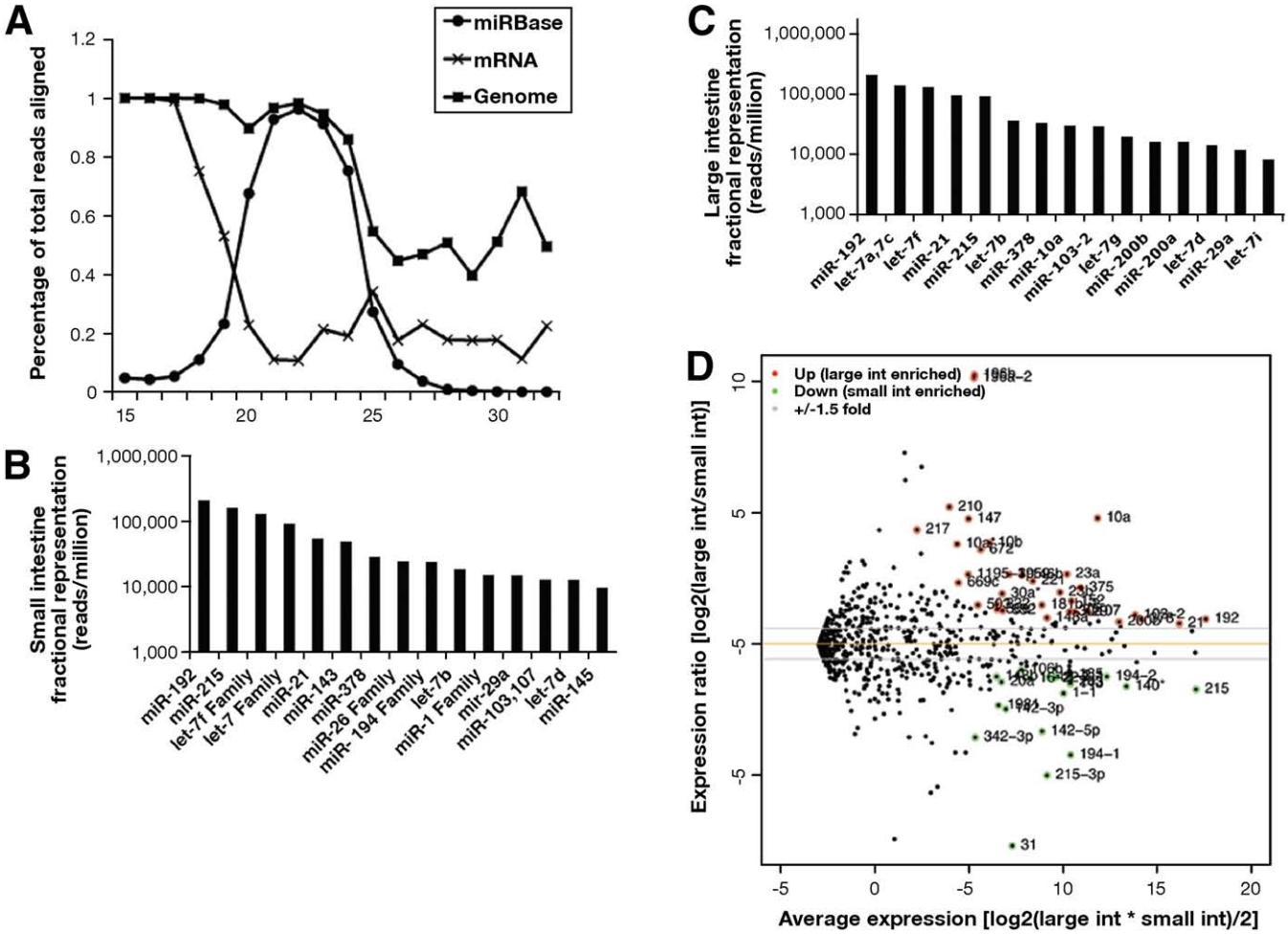

Figure 1. The miRNA transcriptome of the mouse intestine. (*A*) Small RNAs between 19 and 25 nucleotides in length align to both miRBase and the mouse genome (mm8) but not to mRNA sequences from RefSeq. (*B* and *C*) The 15 most abundant miRNAs in jejunal and colonic mucosa. (*D*) Comparison of expression levels of miRNAs in jejunum and colon. Colon-enriched miRNAs are noted with *red dots* and jejunum-enriched with *green dots*.

13,099,974 reads were mapped uniquely to RefSeq mRNAs. There were 1762 regions located in 3′UTRs of mRNAs that were covered by 10 or more reads. We tabulated the frequency of all 6mers found in these regions and determined the significance of their enrichment by comparing the actual observed frequencies to the frequencies observed in 1000 sets of randomly selected 3′UTR regions. A 6mer was considered significant if it was more frequent in fewer than 10 (P value = 10/1000 = 0.01) of the random samples. We then matched the significant 6mers to the seed region of the mature miRNA sequence to identify potential miRNA regulators.

Results

We quantified small RNAs from jejunal and colonic mucosa of adult wild-type mice using ultrahigh throughput sequencing. We aligned the resulting sequence reads to known miRNA precursor genes obtained from miRBase.[16] Next, we verified that these sequence reads represented miRNAs and not degraded mRNAs by aligning them to the RefSeq database. As shown in Figure 1*A*, less than 20% of reads in the miRNA size range aligned to mRNAs, whereas more than 90% matched precursor miRNAs, indicating that our small RNA preparations were highly enriched for true miRNAs. In total, we generated 15.3 million trimmed reads for the small and 47.7 million for the large intestine mucosa. Using these reads, we found evidence for expression of 545 of the 1094 (55.4%) known or predicted mature miRNAs in the jejunal mucosa and 582 (53.2%) in the large intestine mucosa. In the jejunum, these reads represent 540 distinct families and cover 339 of 574 (59.1%) known pre-miRNAs (Figure 1*B*, Supplementary Table 1). In the large intestine, they represent 577 families and cover 357 (62.2%) pre-miRNAs (Figure 1*C*, Supplementary Table 1). We confirmed expression of mmu-miR-194 in both small and large intestinal epithelium via in situ hybridization (Supplementary Figure 1). Included in the miRNA families expressed in the intestinal mucosa are those with known functions in intestinal disease, such

as miR-192, and the miR-200 and let-7 families (Figure 1*B* and *C*).[7,18,19]

There was a strong correlation between the miRNA expression profiles of the small and large intestine (Figure 1*D*). A vast majority (514, 83.8%) of the 613 miRNAs expressed were found in both tissues. In the jejunum, mmu-miR-31 was the most highly enriched gene with a 210-fold change, whereas mmu-miR-196b was enriched in the large intestine by 1231-fold (Figure 1*D*). This suggests that specific miRNAs play unique roles in different portions of the intestinal epithelium, and it will be interesting to investigate the basis of their differential regulation. The sensitivity of the technology used allowed us to detect miRNAs present in a few copies per million as well as those that individually contribute up to ~30% of the total miRNA pool, ie, mmu-miR-192. Because of technical limitations of prior efforts, many of the miRNAs identified here had been missed previously.[10] Because the intestinal epithelium is made up of multiple cell types, without detailed in situ hybridization analysis for all 613 intestinal miRNAs, we cannot determine whether they are expressed uniformly or whether they are expressed at high levels in rarer cell types such as enteroendocrine cells. Nevertheless, our miRNA atlas of the intestinal mucosa dramatically extends prior knowledge in this field.

Next, we wanted to determine to what degree miRNAs contribute to the differentiation and function of the intestine. We derived mice lacking functional miRNAs in the intestinal epithelium by crossing *Dicer1*$^{loxP/loxP}$ conditional mutant mice to *Villin*-Cre mice.[4,11] Quantitative PCR analysis confirmed the deletion of *Dicer1* in the jejunal mucosa at both 3 and 10 weeks of age (Figure 2*A*). In addition, we confirmed the ablation of *Dicer1* at the functional level by determining the abundance of 2 intestinal miRNAs, mmu-miR-21 and mmu-let-7b, via quantitative PCR (Figure 2*A*). Both were dramatically but not completely reduced, reflecting residual *Dicer1* and miRNA expression in cell populations where the *Villin*-Cre transgene is silent, such as mesenchymal or immune cells. Collectively, these results indicate that *Dicer1* was efficiently ablated in the intestinal epithelium of *Dicer1*$^{loxP/loxP}$;*Villin*-Cre mice.

Dicer1$^{loxP/loxP}$;*Villin*-Cre mutants appeared normal at birth and were born in the expected Mendelian ratio. *Dicer1*$^{loxP/+}$;*Villin*-Cre mice displayed no abnormal phenotype. Mutant mice fed normally but were significantly smaller than their littermate controls beginning at 10 days after birth (Figure 2*B* and *C*). This growth impairment continued through weaning (p21). After approximately 2 weeks on chow, mutants began to catch up in weight with their control littermates, becoming indistinguishable in size by 7 weeks of age (Figure 2*B*). In conjunction with impaired growth, preweaned pups had noticeably pale and loose stool. Oil-red-O staining on fecal smears from preweaned (p19) mutants showed the presence of large fat droplets (Figure 2*D*). Once weaned and subsisting on chow, which has only 13.5% kcal from fat as compared with the 80% kcal from fat in mouse milk, mutant feces normalized (data not shown). However, when placed on a "Western Diet" of 45% kcal from fat, *Dicer1* mutants again had markedly increased levels of fat in their stool as compared with controls (Figure 2*D*). Thus, *Dicer1*$^{loxP/loxP}$;*Villin*-Cre mutants cannot process dietary triglycerides. In addition, adult mutants have ~20% higher percent mass of water in their stool as compared with controls (Figure 2*E*).

The *Dicer1*-deficient intestine differed from that of controls morphologically. In the small intestine, there was increased lymphocyte infiltration in the lamina propria of 10-week *Dicer1* mutants, in particular near the crypt zone, as compared with controls (Figure 3*A*). In the colon, the regular crypt structure was disorganized in *Dicer1*-deficient mice, and a more densely packed lamina propria was present between crypts (Figure 3*B*). Whereas Paneth and enteroendocrine cells were present in normal numbers in *Dicer1* mutants (data not shown), the mutants had fewer goblet cells at both 3 weeks (Figure 3*F*) and 10 weeks of age (Figure 3*C–E*), as shown by Alcian blue staining. This decrease was most pronounced in the colon of *Dicer1* mutants (Figure 3*E* and *F*).

There was also a drastic increase in the number of apoptotic epithelial cells in the lower crypt zone of the entire intestine of both 3-week-old (Supplementary Figure 2) and 10-week-old (Figure 4*A* and *B*) *Dicer1* mutants as shown by terminal deoxynucleotidyl transferase-mediated deoxyuridine triphosphate nick-end labeling (TUNEL) staining, whereas apoptotic cells were extremely rare in the healthy intestinal epithelium (Figure 4*A* and *B*). Careful quantification of TUNEL-positive epithelial cells uncovered a significant increase of apoptotic cells in the entire gut at 3 weeks of age (Figure 4*C*). Because of the severe disorganization of the epithelium, accurate quantification of TUNEL-positive epithelial cells was not possible at later stages; however, apoptosis was still present.

We found crypt expansion and increased epithelial cell migration rates in *Dicer1* mutants. Immunohistochemical detection of bromodeoxyuridine (BrdU) incorporation 24 hours after a BrdU pulse showed an increase in proliferating cells higher up on the crypt-villus axis in mutants as compared with controls (Figure 4*D*). Comparison of the leading edge of BrdU-positive cells at 1 hour and 24 hours postinjection allows for calculation of epithelial cell migration rate. In *Dicer1* mutants, epithelial cells of the jejunum migrate 35% faster than those in the control (Figure 4*D*), likely contributing to the disorganization and dysfunction of the mutant epithelium.

Next, we aimed to link the intestinal phenotype of *Dicer1*-mutants to dysregulation of specific classes of mRNAs. Whereas miRNAs affect protein translation, they often also regulate mRNA abundance.[1] We em-

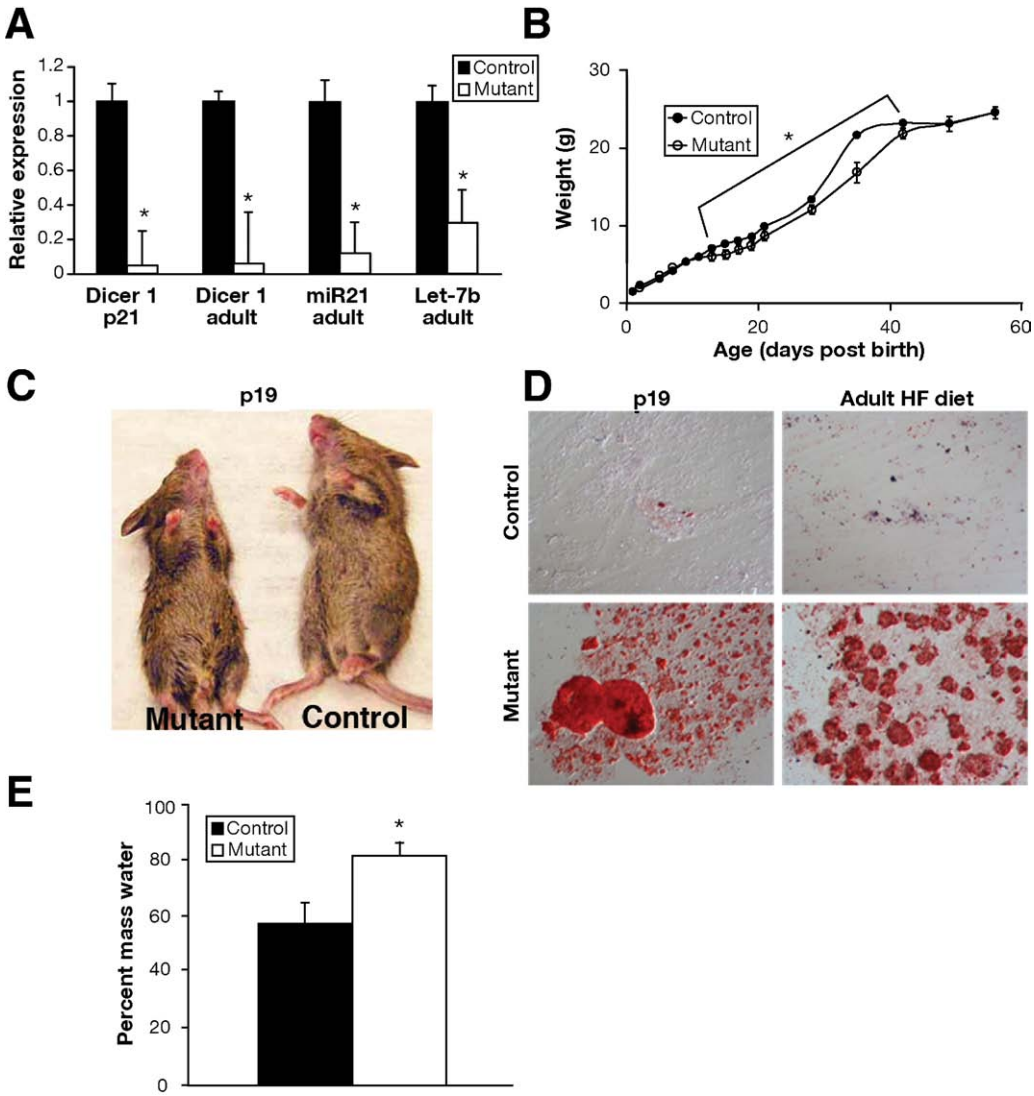

Figure 2. Mice with conditional ablation of *Dicer1* in the intestinal epithelium display impaired growth, fat absorption, and water retention. (*A*) Cre/loxP-mediated gene ablation of *Dicer1* was verified by expression analysis of Dicer1, mmu-miR-21, and mmu-Let-7b in control (*Dicer1*$^{loxP/+}$) and mutant (*Dicer1*$^{loxP/loxP}$;*Villin*-Cre) mice (*$P < .05$). (*B*) *Dicer1* mutants are significantly growth retarded from 10 to 50 days of age but regain weight thereafter (n = 28) (*$P < .05$ by multivariant analysis of variance). (*C*) Size comparison of representative preweaned (*p19*) mutant and control littermates. (*D*) Oil-Red-O staining of fecal smears showing fatty stool in mutant pups preweaning (*p19*) and adult mutants on high-fat chow as compared with controls. (*E*) *Dicer1* mutants fail to absorb water in the colon, as evidenced by the increased water content of their stool compared with control littermates (*$P < .05$).

ployed microarray analysis to identify differentially expressed protein-coding genes. We identified 3156 differentially expressed genes in the jejunal mucosa of *Dicer1* mutants (Supplementary Table 2), which we grouped into functional categories (Figure 5*A*, Supplementary Figure 3).[20] Surprisingly, differentially expressed genes in immune pathways were the largest category of genes affected in *Dicer1*-deficient mice (Figure 5*A*), which we decided to investigate further.

An important component of intestinal defense against luminal pathogens are neutrophils in the lamina propria. H&E staining showed an increase in the number of neutrophils in the lamina propria in both the small and large intestine, with a more dramatic phenotype in the colon (Figure 2*A–D*). Low magnification images demonstrate a dramatic increase in lymphoid nodules in the colon of *Dicer1* mutants (Figure 5*B*). There was an increase in neutrophil number in the lamina propria at the base of the crypts, in addition to a small number seen infiltrating the colonic epithelium, suggesting mild chronic colitis (Figure 5*C*).

To investigate potential causes for the redistribution and increase in immune cells in *Dicer1*-deficient mice, we next analyzed epithelial maintenance in the small intestine of the mutants. In controls, epithelial nuclei were aligned equidistant to the apical surface (Figure 5*D*, *left*, *blue*). This was not the case, however, in *Dicer1* mutants, where the epithelial layer was disorganized and the nuclei were distributed on different planes throughout the ep-

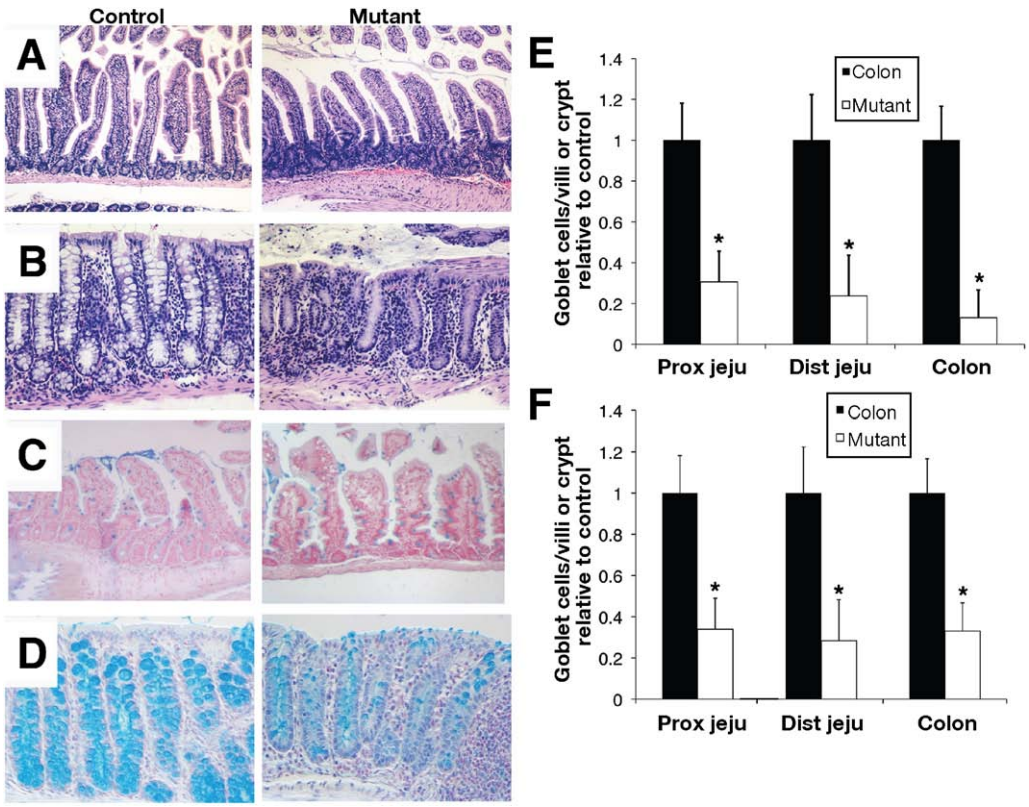

Figure 3. *Dicer1* mutants display increased lymphocyte infiltration and fewer goblet cells throughout the intestine. Adult *Dicer1* mutants (*A*, *right*) display increased cellular density in the crypt zone of the small intestine as compared with littermate controls (*A*, *left*), most likely because of lymphocyte infiltration. Colonic crypts of adult *Dicer1* mutants (*B*, *right*) are disorganized compared with control mice (*B*, *left*). There is a decrease in goblet cells, as shown by Alcian blue staining (*C* and *D*), throughout the intestine in *Dicer1* mutants at 10 weeks (*E*) and 3 weeks (*F*), most notably in the colon, where there is a 4-fold decrease (*$P < .05$).

ithelium (Figure 5*D*, *right*, *blue*). High-resolution confocal imaging of Claudin-7, a component of tight junctions, showed the protein localized to puncta along the basolateral and intracellular membranes of epithelial cells in control intestine (Figure 5*D*, *left*, *red*). In the *Dicer1* mutants, this regular pattern of Claudin-7 staining was lost, again demonstrating the disorganization of *Dicer1*-deficient epithelium (Figure 5*D*, *right*, *red*). Claudin-4, another component of tight junctions, was expressed in clear puncta that lined the apical membrane in the control jejunum (Figure 5*D*, *left*, *green*). In contrast, in *Dicer1* mutants, Claudin-4 puncta were no longer strictly localized to the apical membrane and appeared less densely packed (Figure 5*D*, *right*, *green*).

To determine the consequence of the observed epithelial disorganization in *Dicer1* mutants, we measured the intestinal paracellular permeability. Lactulose and mannitol are nondigestable carbohydrates that cross the epithelium via paracellular routes and are thus useful tools to measure intestinal barrier function.[21] We fed radioactively labeled mannitol and lactulose to 3-month-old mice by gastric gavage and determined their rate of transfer to circulation. Epithelial crossing of both lactulose (Figure 5*E*) and mannitol (Figure 5*F*) was dramatically increased in *Dicer1*-deficient mice, indicative of decreased intestinal epithelial barrier function.

From the severe phenotype of *Dicer1* mutants, it is clear that miRNAs play a vital role in the intestinal mucosa; however, the role of particular miRNAs cannot be deduced from this mouse model. To investigate the roles of specific miRNAs and the mRNAs that they target, we undertook HITS-CLIP for Argonaute, which is an integral part of the RISC that mediates miRNA action.[17] This method involves isolating the jejunal mucosa, immediately cross-linking the protein components of the RISC to the paired miRNA and mRNA simultaneously, isolating these RNA species by immunoprecipitation of Argonaute, and subjecting them to ultrahigh throughput sequencing (Figure 6*A* and *B*). Although most models of miRNA function cite seed sequence binding at the 3′UTR of the target mRNA, our data demonstrate that miRNAs can bind throughout the transcript, although seed sequence binding was enriched within the 3′UTR (Figure 6*C*).[17]

We identified hexamers enriched in 1762 Ago target regions located in Refseq 3′UTRs and matched these to the seed regions of 27 known miRNAs (Supplementary Table 3). mmu-miR-145 seed sequences (ACTGGA) were

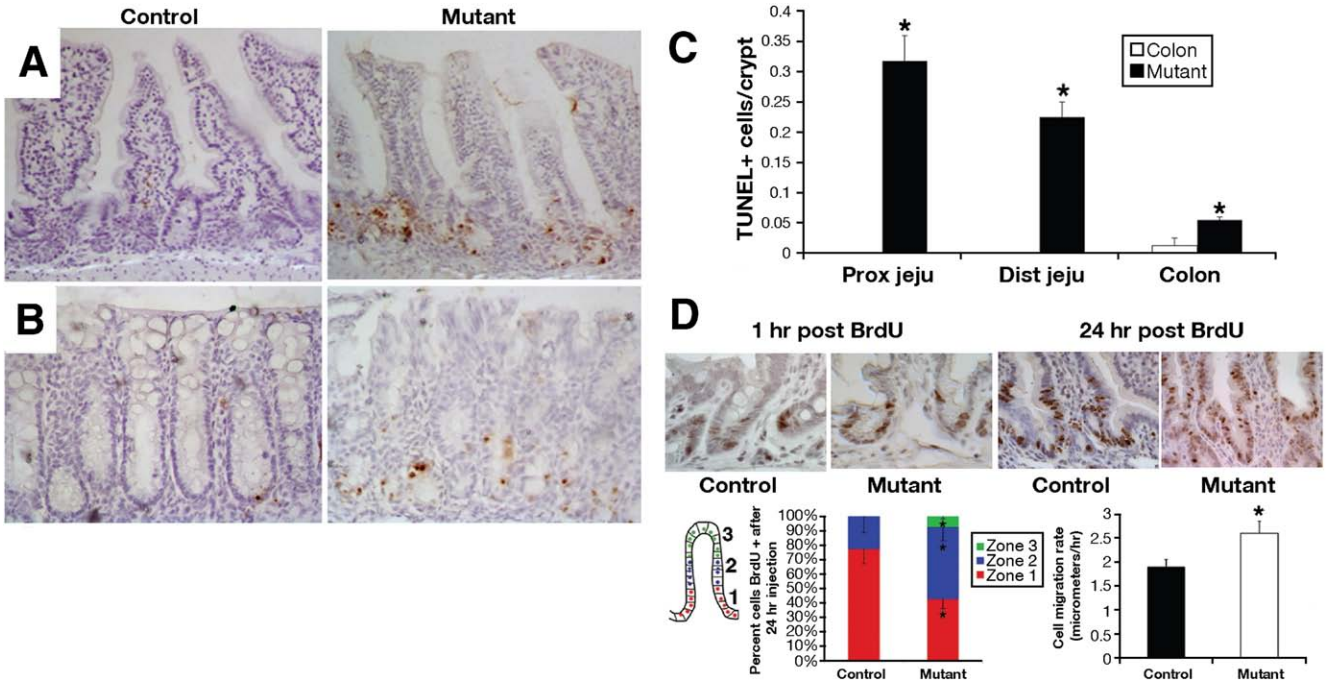

Figure 4. Epithelial cell dynamics in the *Dicer1*-deficient intestine. Epithelial cell apoptosis is increased in *Dicer1* mutants compared with controls at both 3 (*C*) and 10 weeks of age (*A* and *B*). Crypt expansion is observed in *Dicer1* mutants as shown by detection of BrdU incorporation 24 hours after a BrdU pulse (*D*). Epithelial cell migration is accelerated by one-third in *Dicer1* mutants as determined by comparison of the leading edge of BrdU cells at 1 and 24 hours postpulse (*D*) (*$P < .05$).

found in 40 of the mRNA targets identified, many of which are plausible contributors to the phenotype of *Dicer1* mutants described above. *Dicer1* mutant mice display impaired goblet cell differentiation, potentially explained by mmu-miR-145's strongly occupied seed sequences in the 3′UTR of Klf4, a master regulator of goblet cell differentiation.[22] Interestingly, mmu-miR-145 is not the only highly expressed miRNA in the small intestinal mucosa that has an occupied seed sequence in the Klf4 3′UTR; mmu-miR-224 (10 reads) also binds to an enriched hexamer in this region (data not shown). Furthermore, the expressed miRNAs mu-miR-182 (74 reads), mmu-miR-350 (49 reads), mmu-miR-361 (44 reads), and mmu-miR-486 (62 reads) have hexamer matches in the occupied regions of the Klf4 gene as well (Supplementary Table 3). *Dicer1* mutants also display impaired epithelial barrier function, likely caused by disorganization of the epithelial layer and junctional complexes (Figure 5*D*–*F*). Two important cell adhesion proteins, Cadherin1 and Epithelial Membrane Protein 1, are targeted by mmu-miR-145 (Figure 6*D*). Another interesting target of mmu-miR-145 is Cathepsin B (Figure 6*D*), a protein that accumulates in patients with inflammatory bowel diseases.[23] Interestingly, inhibition of Cathepsin B led to amelioration of colitis symptoms.[23] In total, we have uncovered 1328 miRNA-mRNA relationships in the jejunal mucosa using HITS-CLIP, a data set that will undoubtedly be a useful tool for future studies of the roles of miRNAs (Supplementary Table 3).

Discussion

By combining the mRNA microarray data with HITS-CLIP-derived targeting information, we can identify a set of miRNA targets whose expression levels are affected in the small intestine by deletion of *Dicer1*, among them the aforementioned Cadherin 1 and Cathepsin B genes (see Supplementary Table 4 for summary). We analyzed transcription factors as potentially important targets because they control transcriptional networks and often play fundamental well-studied roles in processes such as development and homeostasis. Table 1 contains 7 transcription factors and signaling molecules that are both up-regulated in *Dicer1* mutants and are high-confidence targets of miRNAs expressed in the jejunal mucosa. Among these are the Reg proteins, originally identified as growth factors for pancreatic β-cells. Regβ and γ are both miRNA targets as determined by HITS-CLIP and up-regulated in *Dicer1* mutants (Supplementary Table 2). Reg3β negatively regulates tumor necrosis factor α-induced nuclear factor-κB activation and therefore plays a role in innate immune response in the intestine.[24,25] Expression of both these genes is regulated by Relmβ levels,[24] a signaling molecule secreted by goblet cells and known to play a role in inflammation and infection susceptibility.[26] Interestingly, Relmβ expression is also up-regulated in *Dicer1* mutants (Supplementary Table 2). Relmβ$^{-/-}$ mice have decreased epithelial resistance and increased epithelial permeability and are also

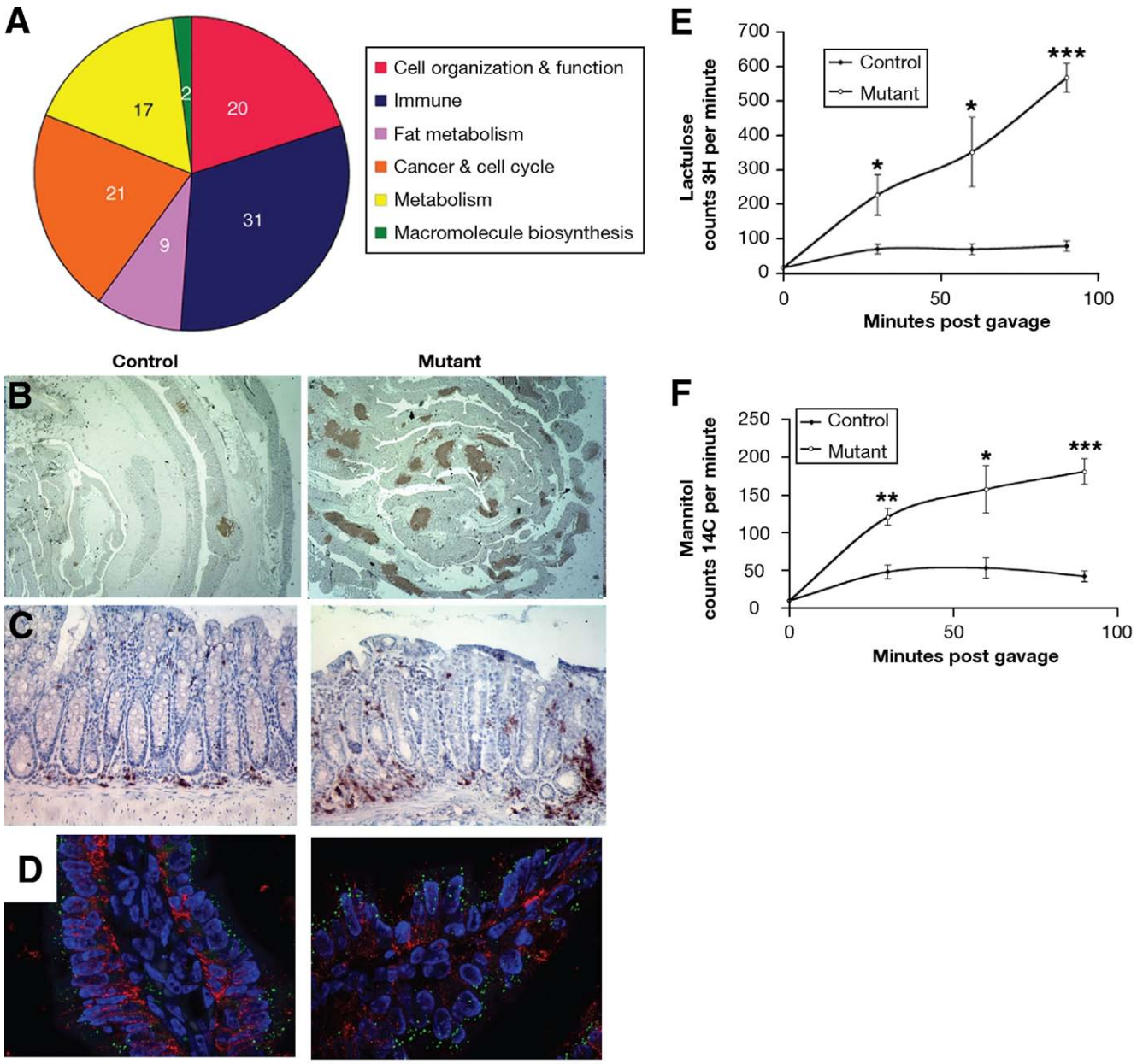

Figure 5. *Dicer1* mutants exhibit increased inflammation because of a disorganized epithelium and decreased tight junctions leading to increased intestinal permeability. (*A*) Gene expression profiles of jejunal mucosa of *Dicer1* mutants and controls were determined. Differentially expressed genes were sorted into pathways, and the differentially activated pathways were combined into functional groups. Immune pathways made up one-third of the differentially expressed genes. (*B*) Low magnification (4×) image of a "Swiss-roll" large intestine stained for B cells (CD45R) shows an increase in the number of lymphoid nodules in mutants as compared with controls. (*C*) *Dicer1* mutants have increased B-cell infiltration as compared with controls. (*D*) The small intestinal epithelium of mutants is disorganized as shown by high-resolution confocal imaging of immunofluorescent staining of Claudin-7 (*red*), Claudin-4 (*green*), and nuclei (*blue*). *Dicer1* mutants have increased intestinal permeability as shown by lactulose (*E*) and mannitol (*F*) absorption (*$P > .05$. **$P > .01$, ***$P > .0001$) (n = 5).

protected from the deleterious symptoms of chemically induced colitis.[24] Taken together, the regulation of these 3 genes by miRNAs is likely involved in epithelial barrier function and innate immune response.

Transcription factor CP2-like1 (Tcfp2l1) is active in pluripotent embryonic stem cells and is down-regulated as cells differentiate.[27] Its role in the intestine may be limited to the stem cell compartment that repopulates the epithelium as cells move up the crypt-villus axis. miRNA targeting of Tcfp211 may be part of the down-regulation of this gene as cells commit to the various intestinal epithelial cell types, and its overexpression in our *Dicer1* mutants might contribute to the observed expansion of the proliferative zone described above.

Hoxb9 is a Wnt/Tcf/Lef target gene that was shown recently to be involved in metastasis of adenocarcinma of

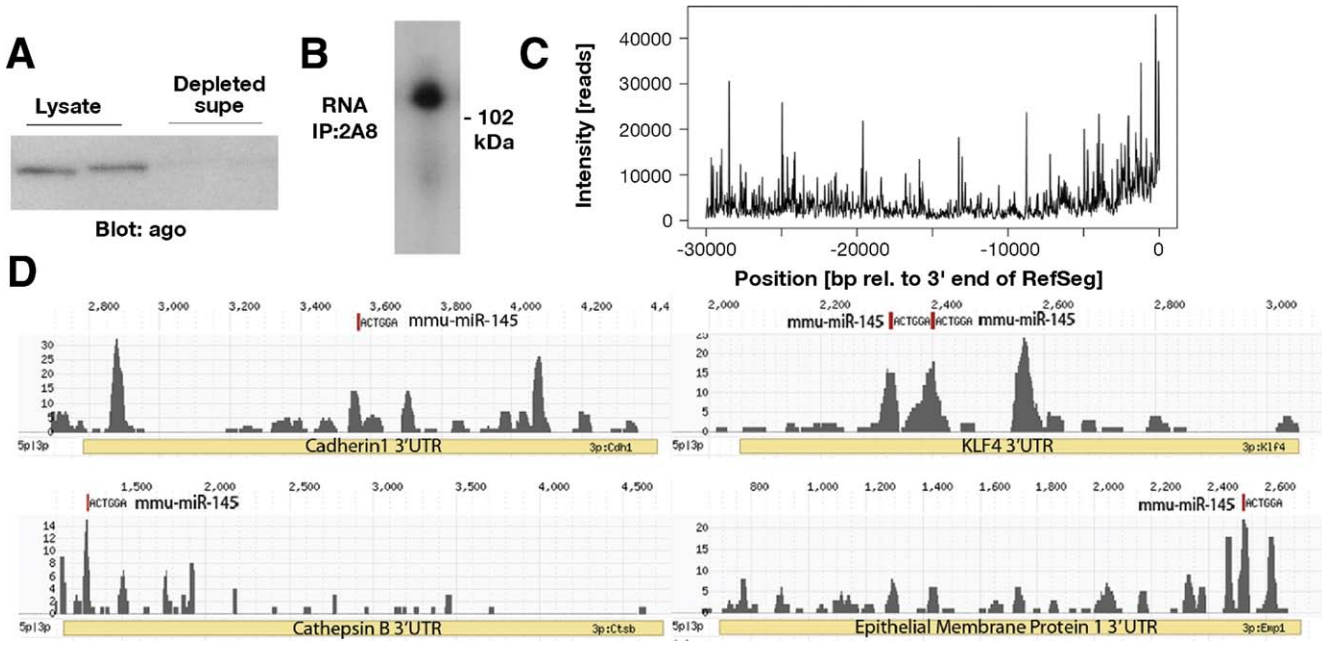

Figure 6. Identification of miRNA targets in the intestinal epithelium. (*A*) Argonaute protein, and the cross-linked RISC, were successfully immunoprecipitated from lysates of jejunal mucosa. (*B*) Along with Argonaute, RNA populations of the expected size were also present in the immunoprecipitated samples. (*C*) While miRNA target sequences obtained from HITS-CLIP were distributed along the length of mRNAs as shown in this summary analysis, there was an enrichment of binding near the end of the 3′UTR. The *graph* depicts the summary for all target sequences within mRNAs obtained from HITS-CLIP. To be able to represent all different mRNAs in 1 graph, the distances were expressed in each case relative to the 3′ end of the respective RefSeq mRNA, which was defined as position 0. The *y-axis* indicates the "intensity" as derived from the number of sequence reads obtained. (*D*) miR-145, one of the most highly expressed miRNAs in the small intestinal epithelium, targets several genes whose misexpression could explain the *Dicer1* mutant phenotype: *Klf4*, *Cadherin1*, *Epithelial Membrane Protein 1*, and *Cathepsin B*. The graphs display the 3′UTR of each gene (*yellow*) box and the sequencing reads of mRNA fragments obtained from the HITS-CLIP experiment for each of the 4 genes (*gray peaks*). At the *top* of each graph is the alignment with the seed sequence of miR-145 (*red box*). Note that the locations of the match to the miR-145 seed sequence coincide with peaks of mRNA fragments obtained from HITS-CLIP analysis.

the lung, an organ that, like the intestine, is derived from embryonic endoderm.[28] Whereas a function for Hoxb9 in the intestine has yet to be described, it is tempting to speculate that its normal repression by miRNAs in the intestine—which is subject to active Wnt signaling in transit amplifying cells—is required for intestinal tissue homeostasis.

Table 1. Transcription Factors and Signaling Molecules Targeted by Intestinal miRNAs and Up-Regulated in *Dicer1* Mutants

Transcription factors and signaling proteins	mRNA fold change	Targeting miRNAs (reads per million)
Tcfcp2l1	5.53	miR-25 (2313), miR-145 (9321)
Reg3g	4.52	miR-23a (1402), miR-23b (876), miR-130a (244), miR-130b (134)
Hoxb9	3.56	mir-150 (105)
Reg3b	2.73	miR-23a (1402), miR-23b (876), miR-805 (909)
Tnfaip3	2.09	miR-31 (1945)
Elf4	1.67	miR-22 (1099)
Onecut2	1.52	miR-33 (139), miR-375 (1244)

NOTE. Seven transcription factors and signaling molecules are listed that are both up-regulated in *Dicer1* mutants and are high-confidence targets of miRNAs expressed in the jejunal mucosa along with the mRNA fold change in *Dicer1* mutants and targeting jejunal miRNAs.

TNFAIP3, also known as A20, is a negative regulator of Toll-like receptor signaling in intestinal epithelial cells as it inhibits nuclear factor-κB.[29] Its expression is rapidly up-regulated in response to immune challenge and gradually declines back to basal levels as the cells or tissue recover.[29] *Dicer1* mutants have substantial tissue damage and immune infiltration, therefore, miRNA targeting of A20 suggests a role of the innate immune system in response to compromised barrier function in these mutants.

ELF-4 controls proliferation of $CD8^+$ T cells by directly activating the tumor-suppressor gene KLF4.[30] Interestingly in NIH3T3 fibroblast cells, over-expression of ELF-4 pushes cells through the G_1/S transition to promote cell cycle entry and proliferation.[31] Because miRNAs are generally thought to decrease expression of their targets, *Dicer1* mutants would have increased levels of ELF-4, potentially explaining the crypt expansion and increased cell migration rate in the small intestinal epithelium.

Onecut 2 (Hnf6β) has been shown to play a role in gut patterning and differentiation of enteroendocrine cells.[32] Whereas there is no direct correlation with the phenotype

of the *Dicer1* mutants and these functions, it is likely that Onecut 2 plays other roles in the intestinal epithelium as well as it is highly expressed throughout the tissue.[32] It has been previously reported that both miR-495 (43.78 reads per million) and miR-218 (25.75 reads per million) regulate Onecut 2 in liver and pancreas,[33] but these 2 miRNAs are expressed at very low levels in the intestine. We predict mmu-miR-33 (166 reads per million) and mmu-miR-375 (2086 RPM) as likely regulators of Onecut 2 in the jejunal mucosa from our HITS-CLIP data and hexamer seed matches (Supplementary Table 3).

In summary, we have established that miRNAs play multiple important roles in the intestinal epithelium. This was not a foregone conclusion because the function of hepatocytes, another endoderm derived cell type, is largely independent of microRNAs.[5] Whereas previous studies have focused on the role of miRNAs in colon cancer, here we show new functional roles for miRNAs in epithelial organization, cell migration, barrier function, and the prevention of colitis. Additionally, we provide the basis for a better understanding of miRNA-mRNA targeting relationships in the intestinal mucosa using HITS-CLIP technology and show that targets of particular miRNAs can be linked to aspects of the phenotype of *Dicer1* mutant mice, thus providing at least part of the molecular mechanism behind miRNA function in the intestinal epithelium.

Supplementary Material

Note: To access the supplementary material accompanying this article, visit the online version of *Gastroenterology* at www.gastrojournal.org, and at doi: 10.1053/j.gastro.2010.07.040

References

1. Bartel D. MicroRNAs: target recognition and regulatory functions. Cell 2009;136:215–233.
2. Lewis BP, Burge CB, Bartel DP, et al. Conserved seed pairing, often flanked by adenosines, indicates that thousands of human genes are microRNA targets. Cell 2005;120:15–20.
3. Bartel D. MicroRNAs: genomics, biogenesis, mechanism, and function. Cell 2004;116:281–297.
4. Cobb BS, Nesterova TB, Thompson E, et al. T-cell lineage choice and differentiation in the absence of the RNase III enzyme Dicer. J Exp Med 2005;201:1367–1373.
5. Hand NJ, Master ZR, Le Lay J, et al. Hepatic function is preserved in the absence of mature microRNAs. Hepatology 2009;49:618–626.
6. Sekine S, Ogawa R, Ito R, et al. Disruption of Dicer1 induces dysregulated fetal gene expression and promotes hepatocarcinogenesis. Gastroenterology 2009;136:2304–2315.
7. Akao Y, Nakagawa Y, Naoe T, et al. let-7 microRNA functions as a potential growth supressor in human colon cancer cells. Biol Pharm Bull 2006;29:903–906.
8. Wu F, Zikusoka M, Trindade A, et al. MicroRNAs are differentially expressed in ulcerative colitis and alter expression of macrophage inflammatory peptide-2a. Gastroenterology 2008;135:1624–1635.
9. Landgraf P, Rusu M, Sheridan R, et al. A mammalian microRNA expression atlas based on small RNA library sequencing. Cell 2007;129:1401–1414.
10. Cummins JM, He Y, Leary RJ, et al. The colorectal microRNAome. Proc Natl Acad Sci U S A 2006;103:3687–3692.
11. Madison BB, Dunbar L, Qiao XT, et al. Cis elements of the villin gene control expression in restricted domains of the vertical (crypt) and horizontal (duodenum, cecum) axes of the intestine. J Biol Chem 2002;277:33275–33283.
12. Gupta RK, Gao N, Gorski RK, et al. Expansion of adult β-cell mass in response to increased metabolic demand is dependent on HNF-4α. Genes Dev 2007;21:756–769.
13. Gao N, Le Lay J, Vatamaniuk MZ, et al. Dynamic regulation of Pdx1 enhancers by Foxa1 and Foxa2 is essential for pancreas development. Genes Dev 2008;22:3435–3448.
14. Gentleman RCV, Huber W, Irizarry R, et al. Bioinformatics and computational biology solutions using R and Bioconductor. Springer, New York, NY: 2005.pp 55–66.
15. Tusher VG, Tibshirani R, Chu G, et al. Significance analysis of microarrays applied to the ionizing radiation response. Proc Natl Acad Sci U S A 2001;98:5116–5121.
16. Griffiths-Jones S, Saini HK, van Dongen S, et al. miRbase: tools for microRNA genomics. Nucelic Acids Res 2003;36:D154–D158.
17. Chi SW, Zang JB, Mele A, et al. Argonaute HITS-CLIP decodes microRNA-mRNA interaction maps. Nature 2009;460:479–486.
18. Hino K, Fukao T, Watanabe M, et al. Regulatory interaction of HNF-1a to microRNA-194 gene during intestinal epithelial cell differentiation. Nucleic Acids Symp Ser 2007;51:415–416.
19. Gregory PA, Bert AG, Paterson EL, et al. The miR-200 family and miR-205 regulate epithelial to mesenchymal transition by targeting ZEB1 and SIP1. Nat Cell Biol 2008;10:593–601.
20. Mootha VK, Lindgren CM, Eriksson KF, et al. PGC-1α-responsive genes involved in oxidative phosphorylation are coordinately down-regulated in human diabetes. Nat Genet 2003;34:267–273.
21. Travis S, Menzies I. Intestinal permeability: functional assessment and significance. Clin Sci (Lond) 1992:471–488.
22. Katz JP, Perreault N, Goldstein BG, et al. The zinc-finger transcription factor Klf4 is required for terminal differentiation of goblet cells in the colon. Development 2002;129:2619–2628.
23. Menzel K, Hausmann M, Obermeier F, et al. Cathepsins B, L, and D in inflammatory bowel disease macrophages and potential therapeutic effects of cathepsin inhibition in vivo. Clin Exp Immunol 2006;146:169–180.
24. Hogan SP, Seidu L, Blanchard C, et al. Resistin-like molecule β regulates innate colonic function: barrier integrity and inflammation susceptibility. J Allergy Clin Immunol 2006;118:257–268.
25. Gironella M, Iovanna JL, Sans M, et al. Anti-inflammatory effects of pancreatitis associated protein in inflammatory bowel disease. Gut 2005;54:1244–1253.
26. Artis D, Wang ML, Keilbaugh SA, et al. RELMβ/FIZZ2 is a goblet cell-specific immune-effector molecule in the gastrointestinal tract. Proc Natl Acad Sci U S A 2004;101:13596–13600.
27. van den Berg DL, Snoek T, Mullin NP, et al. An Oct4-centered protein interaction network in embryonic stem cells. Cell Stem Cell 2010;6:329–381.
28. Nguyen DX, Chiang AC, Zhang XH, et al. WNT/TCF signaling through LEF1 and HOXB9 mediates lung adenocarcinoma metastasis. Cell 2009;138:51–62.
29. Oshima N, Ishihara S, Rumi MA, et al. A20 is an early responding negative regulator of Toll-like receptor 5 signalling in intestinal epithelial cells during inflammation. Clin Exp Immunol 2010;159:185–198.
30. Yamada T, Park CS, Mamonkin M, et al. Transcription factor ELF4 controls the proliferation and homing of CD8+ T cells via the

Krüppel-like factors KLF4 and KLF2. Nat Immunol 2009;10:618–626.
31. Liu Y, Hedvat CV, Mao S, et al. The ETS protein MEF is regulated by phosphorylation-dependent proteolysis via the protein-ubiquitin ligase SCFSkp2. Mol Cell Biol 2006;26:3114–3123.
32. Vanhorenbeeck V, Jenny M, Cornut JF, et al. Role of the Onecut transcription factors in pancreas morphogenesis and in pancreatic and enteric endocrine differentiation. Dev Biol 2007;305:685–694.
33. Simion A, Laudadio I, Prévot PP, et al. miR-495 and miR-218 regulate the expression of the Onecut transcription factors HNF-6 and OC-2. Biochem Biophys Res Commun 2010;301:293–298.

Received October 21, 2009. Accepted July 21, 2010.

Reprint requests

Address requests for reprints to: Klaus H. Kaestner, PhD, Department of Genetics and Institute for Diabetes, Obesity, and Metabolism, University of Pennsylvania School of Medicine, Philadelphia, Pennsylvania 19103. e-mail: Kaestner@mail.med.upenn.edu.

Acknowledgments

The authors thank Drs Merkenschlager, Gumucio, Rustgi, and Mourelatos for reagents; Elizabeth Helmbrecht and Karrie Brondell for maintenance of the mouse colony; Amber Horner for technical assistance; Dr Gary Swain, Jaclyn Twaddle, and the entire morphology core of the Penn Center for Molecular Studies in Digestive and Kidney Disease (DK-050306) for reagents and technical assistance; Dr Marie Hildebrandt, Markiyan Doliba, and Christopher Morgan for technical assistance; and Dr John Le Lay for critical reading of the manuscript.

Conflicts of interest

The authors disclose no conflicts.

Funding

Supported by T32-HD007516 (to L.B.M.) and NIDDK grant R01-DK053839 (to K.H.K.).

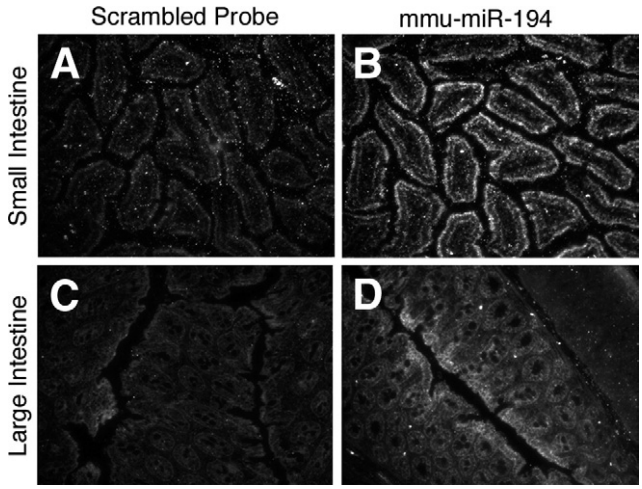

Supplementary Figure 1. In situ hybridization confirms mmu-miR-194 expression in both the small and large intestinal epithelium. In situ hybridization using both a scramble probe as a control (*A* and *C*) and a probe for mmu-miR-194 (*B* and *D*) shows clear epithelial miRNA expression in both the small (*B*) and large (*D*) intestine in a wild-type mouse.

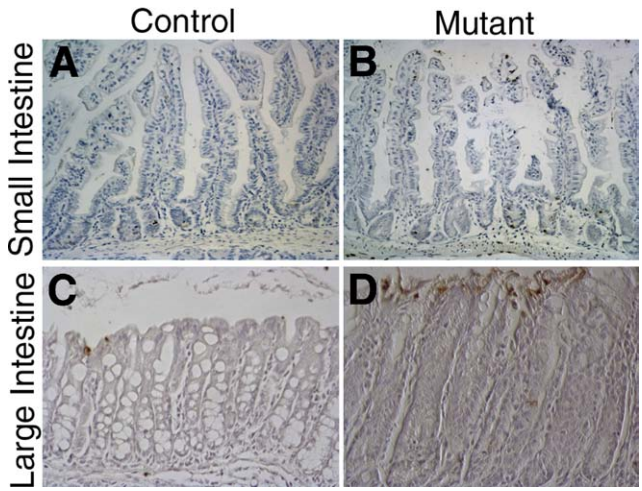

Supplementary Figure 2. Increased apoptosis in the small and large intestine of 3-week-old *Dicer1* mutant mice. Apoptotic epithelial cells, as shown by terminal deoxynucleotidyl transferase-mediated deoxyuridine triphosphate nick-end labeling staining, are increased in the epithelium of 3-week-old *Dicer1* mutants (*B* and *D*) as compared with controls (*A* and *C*) in both the small and large intestine.

Category	Upregulated	FDR (%)	Downregulated	FDR (%)
Immune	Natural Killer Cell Mediated Cytotoxicity	.5	Regulation of Autophagy	.4
Cancer & Cell Cycle	_____	___	Cell Cycle	0
Cell Org. & Function	_____	___	Glycan Structures Degradation	1
Metabolism	Metabolism of Xenobiotics	.008	Aminosugars Metabolism	.2
Fat Metabolism	Bile Acid Biosynthesis	22	Ether Lipid Metabolism	24
Macromol. Biosynthesis	_____	____	Alkaloid Biosynthesis	9

Supplementary Figure 3. The most highly up- and down-regulated Kyoto Encyclopedia of Genes and Genomes (KEGG) pathways in each of the categories used in *Dicer1* mutants. Enriched KEGG pathways were identified using gene set enrichment analysis (*GSEA*), and the genes were grouped into categories. The most highly up- and down-regulated pathways in each category are listed, along with its false discovery rate (*FDR*).